

Imaging Microwave Response of rf-SQUID Metasurface in dc Magnetic Field

Alexander P. Zhuravel

B. Verkin Institute for Low Temperature Physics & Engineering (ILTPE)
National Academy of Science of Ukraine (NASU)
UA-61103 Kharkov, Ukraine
zhuravel@ilt.kharkov.ua

Alexey V. Ustinov

Physikalisches Institute
Karlsruhe Institute of Technology (KIT)
76131 Karlsruhe, Germany
National University of Science and Technology (MISIS)
119049 Moscow, Russia

M. Trepanier, Daimeng Zhang and Steven M. Anlage

CNAM, Physics Department
University of Maryland
College Park, Maryland 20742-4111, USA

Abstract— We report direct visualization of spatially localized excitations in an array of 27x27 coupled rf-SQUIDs forming a magnetic meta-surface for electromagnetic wave propagation. The technique of low-temperature Laser Scanning Microscopy (LSM) is applied to investigate contributions of individual meta-atoms to the macroscopic dc flux tuned microwave response in the high rf flux limit. The obtained LSM images of the RF current distributions across the SQUID array at zero dc flux confirms a high degree of coherence of the entire meta-surface assuming radially anisotropic nearest neighbor coupling in 2D arrays of rf-SQUIDs. We also find a rich variety of spatially clustered stable dissipative states of the rf-SQUID array due to the non-uniform penetration of magnetic flux in the direction perpendicular to the uniform external magnetic field. Our measurements show that the LSM technique is a powerful tool for spatially-resolved characterization of complicated meta-materials and may be useful for their optimization.

Keywords— Josephson junctions; microwave metamaterials; superconducting quantum interference devices (SQUIDs); superconductors; superconducting electronics; laser scanning microscopy (LSM)

I. INTRODUCTION

A magnetic rf meta-surface refers to a kind of engineered planar structure with sub-wavelength thickness and strong negative magnetic susceptibility unachievable in natural materials [1]. These are generally created by assembling arrays of miniature unit cells (magnetic meta-atoms) such as split-ring (SRR) and spiral-like resonators operating at microwave or higher frequency bands [2]. Since the typical design is supported with normal metals, ohmic losses and bulkiness are the limiting factors. Therefore, superconducting Nb and $\text{YBa}_2\text{Cu}_3\text{O}_{7-\delta}$ meta-atoms were realized alternatively with some success combining their intrinsic advantages of low-loss, large inductance (with the addition of kinetic inductance), and tunability compared to their normal metal

counterparts [3, 4]. Recently, a new generation of the superconducting meta-atoms was implemented based on an rf-SQUID that incorporates a Josephson junction (JJ) instead of the capacitance gap in the SRR.

The benefits of an rf SQUID meta-atom were presented theoretically in [5-7] showing that the self-resonance frequency can be precisely changed by temperature and rf current without a substantial increase in losses, realized by means of the intrinsically tunable Josephson inductance [8-10]. In addition, the magnetic field tunability of the resonance frequency of such a flux-controlled rf-SQUID meta-atom has been experimentally verified [8, 11]. Even more intriguing facts have manifested themselves in the study of the rf-SQUID based meta-surfaces. A novel transparency behavior for intermediate values of rf flux have been demonstrated [12]. Spatially dynamic Chimera states [13] and spatially-kaleidoscopic magneto-inductive modes [8, 14] have been theoretically predicted assuming homogenous dc and rf applied fields.

Therefore it is highly desirable to develop methods of spatially-resolved analysis capable not only to visualize the coherent response of the rf-SQUID array but also to verify the validity of the theoretical predictions. The Laser Scanning Microscopy (LSM) technique has been employed in the past to image coherent response in arrays of strongly coupled rf-SQUIDs [15]. In this research we are focused on investigation rf-SQUID system with a magnetically destroyed coupling that meets the requirements of the statement mentioned above. The preliminary objective of the proposed investigation was to test LSM capability using obviously predictable pattern of rf-SQUID response in the high rf flux limit. This regime is predicted to show spatially homogenous response of all superconducting unit cells at the frequency of the geometric resonance f_{geo} independent of dc flux at temperatures well below T_c . Surprisingly, a few more resonances were found to extend our LSM study toward understanding the local origin

This work is supported by the NSF-GOALI and OISE programs through Grant No. ECCS-1158644 and CNAM; Partial support by the Ministry of Education and Science of Russian Federation in the framework of Increase Competitiveness Program of the NUST MISIS (contracts no. K2-2014-025 and K2-2015-002) as well as the support of the Volkswagen Foundation are gratefully acknowledged.

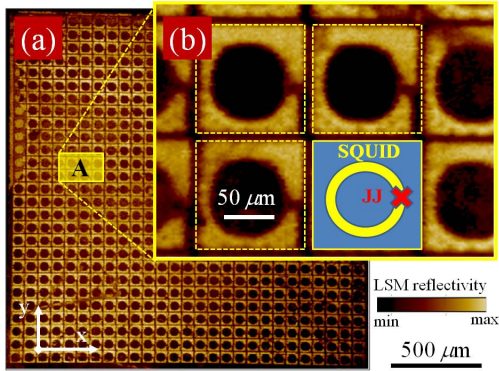


Fig. 1. Two-dimension LSM reflectivity map of 27x27 rf-SQUID array showing (a) whole area of the sample along with (b) detailed view of individual unit cells in area A that outlined by yellow dashed boxes. Schematic drawing of a single SQUID per cell is shown in the inset.

of spatial rf-SQUID array incoherence produced by weak dc magnetic field.

II. EXPERIMENTAL DETAILS

A. Sample

The meta-surface under test was a regular array of 27x27 rf-SQUIDs whose microwave design, global experimental characterization and detailed simulation has been described in [8]. The structure was made on an SiO₂ substrate using the standard HYPRES fabrication process of Nb/AlO_x/Nb trilayer Josephson tunnel junctions (JJs) with their critical current densities of about 0.3 $\mu\text{A}/\mu\text{m}^2$ at 4.2 K [16]. Fig. 1(a) shows the optical reflectance LSM image collected over the area of all 27x27 unit cells of presumably identical rf-SQUIDs separated with a center-to-center distance of 83 μm . A schematic drawing of a single SQUID per cell is shown in Fig. 1(b) which demonstrates an enlarged fragment of the array for a better comparison. As has been discussed in [8], tunability is the crucial design parameter of the SQUID, and it should allow precise adjustment of the meta-surface resonance within the measurable frequency range 8–20 GHz (dictated by the available waveguide) while remaining in the low noise and non-hysteretic limits [17]. This may be controlled by choice of the inner and outer radii of the loop and thus the loop inductance L , the critical current I_c of the JJ, and the overlap capacitance C . In the investigated design, the inner and outer radii of the SQUID loops are 30 and 40 μm , respectively. The estimated L is 0.12 nH, and the area of the JJ and the area of the capacitor are 13 and 1800 μm^2 , respectively, yielding nominal design values of $I_c(4.2 \text{ K}) = 3.7 \mu\text{A}$ and $C = 0.84 \text{ pF}$ [8, 10].

The sample is placed in the center of a rectangular waveguide on a cold quartz rod orienting the planar structure of the silicon chip with the SQUID array orthogonally to the magnetic component of the exciting rf field almost homogenous over the area of the meta-surface (see Fig. 2). Additionally, we can apply a homogenous dc magnetic flux via a set of superconducting Helmholtz coils outside the waveguide. The whole construction is surrounded by a mu-

metal magnetic shielding and temperature stabilized in the range between 4.5 and 10 K with an accuracy of 1 mK. The effectiveness of this setup in LSM research of superconducting meta-surfaces has recently been demonstrated [18].

B. LSM technique

In our current work we pursue a direct way to image local resonances of spatially distributed rf-SQUIDs in the array by using the method of laser scanning microscopy (LSM). The LSM technique can measure the optical and rf properties in an area of the superconducting meta-surface devices simultaneously and is ideally suited for studying the spatial location of the resonating unit cells in the area of the rf-SQUID array. The LSM uses the principle of raster scanning the surface of the examined structure by a laser probe. This occurs by focusing the laser beam onto the surface of the rf-SQUID array through a hole in the waveguide which is cooled in the vacuum cavity of the optical cryostat. The (i) reflected laser radiation is detected as a function of probe coordinate x , y to visualize in-plane positions and geometry of the unit cells (see Fig. 1). The (ii) absorbed light quanta heats the sample on the thermal healing length scale l_T for bolometric probing of all the thermo-sensitive properties of the meta-surface that change the microwave transmittance $S_{21}(f)$ through the waveguide. The laser intensity is modulated at 100 kHz, and the changes in rf transmission at a fixed frequency are phase sensitively detected, resulting in a photo-response (PR) signal. This is produced due to a slight shift of the resonance frequency of that SQUID which is illuminated. In this case, the thermally (δT) - induced modulation of $S_{21}(f)$ underneath the probe results in PR, and can be expressed as $\text{PR} \sim [d||S_{12}(f)||^2/dT]\delta T$.

In particular, modulation of kinetic and Josephson inductance by a thermal probe allows one to measure a quantity proportional to $A\lambda_{\text{eff}}^2(x, y)J_{\text{rf}}^2(x, y)\delta\lambda_{\text{eff}}$, and consequently can be used for extraction of $J_{\text{rf}}^2(x, y)$ maps [19–21]. Here $\delta\lambda_{\text{eff}}$ is the photo-induced change in effective magnetic penetration depth λ_{eff} ($\sim\lambda_{\text{JJ}}$), and A is the area of the exciting spot (related to both $l_T \sim 5 \mu\text{m}$ and diameter of the

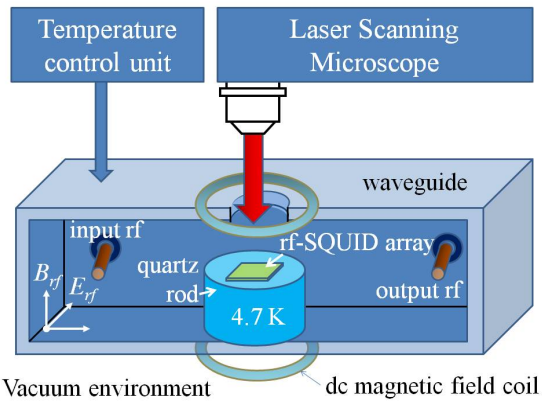


Fig. 2. Schematic of the microwave LSM experiment. rf-SQUID metasurface is positioned inside a waveguide perpendicular to rf magnetic field. The dc magnetic field is created by two superconducting coils outside the waveguide.

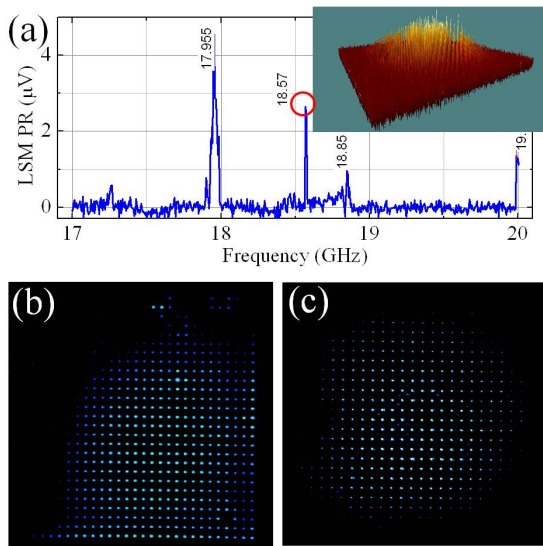


Fig. 3. (a) Frequency dependence of LSM PR measured at position of a single Josephson junction located in the center of 27x27 rf-SQUID array. 2D images show PR(x, y) distribution at resonances of (b) 17.955 GHz and (c) 18.57 GHz at $P_{rf} = -20$ dBm, $P_L = 10 \mu\text{W}$; $T = 4.7$ K and zero dc flux. The inset shows a 3D image of (c).

optical probe $\sim 10 \mu\text{m}$). We expect that PR distribution in the rf-SQUID array magnitude should demonstrate a regular pattern of 27x27 peaks located just at the JJs producing maximum response at $f = f_{geo}$ due to modulation of the Josephson inductance. Thus, rastering the laser probe across the area of 27x27 rf-SQUIDS and gray-scale-encoding the magnitude of the LSM photoresponse as a function of the beam position, one can reveal a two-dimensional picture which maps the magnetically inductive state of the whole array at a certain value of the external dc magnetic field, circulating microwave power and resonant frequency. For more details on the LSM technique, see [22].

III. RESULTS AND DISCUSSION

We proceed from the assumption [8, 12] that the only detectable mode of the rf-SQUID array in the high rf flux limit is a geometrical resonance. It is precisely this regime that is realized at $P_{rf} = -20$ dBm corresponding to the requirements of $\log(\Phi_{rf}/\Phi_0) > -1$, where the tunable resonant frequency reduces to a fixed value, as postulated in [8]. Surprisingly, a few other magneto-inductive modes were LSM visualized. Figure 3(a) shows the local LSM response of a single Josephson junction located in the middle of the SQUID array. Photoresponse is measured as function of rf frequency at fixed position of the laser probe. At least three resonant peaks are evident. The $PR(x,y)$ at $f = 17.955$ GHz in Fig. 3(b) is a coherent response at the geometric resonance showing spatial anisotropy of the photo-response: Black areas in the upper left area correspond to positions of SQUIDs that are out of resonance. In addition, several discrete breather-like clusters of rf-SQUIDS [23] are still visible in this area. Those clusters look like grouped bright points in the black background.

Further, clustering is accompanied by increased dissipation, under the influence of stray dc magnetic flux, as

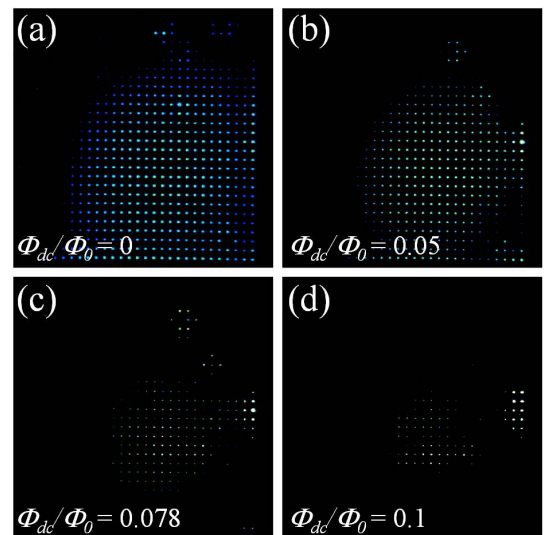


Fig. 4. 2D LSM images of 27x27 rf-SQUID array photoresponse probed at $P_{rf} = -20$ dBm, $P_L = 10 \mu\text{W}$; $T = 4.7$ K in dissipative mode of geometric resonance $f_{geo} = 17.955$ GHz at different reduced dc fluxes Φ_{dc}/Φ_0 of (a) 0, (b) 0.05, (c) 0.078 and (d) 0.1.

seen in Fig. 4. The response of the SQUID array diminishes progressively to the point of disappearance at reduced dc flux $\Phi_{dc}/\Phi_0 > 0.1$, where Φ_0 is the flux quantum. In contrast, another magneto-inductive mode generates expected coherent

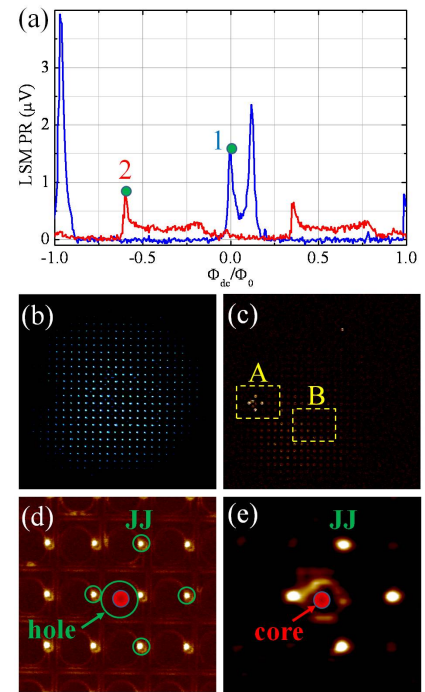


Fig. 5. (a) Plot of PR amplitude vs. Φ_{dc}/Φ_0 measured at fixed position of the laser probe on a center JJ of the rf-SQUID array that is zero-field (curve 1) and non-zero (curve 2) cooled in the temperature range from $T > T_c$ down to $T = 4.7$ K $P_{rf} = -20$ dBm along with corresponding 2D LSM images (b) and (c). Enlarged LSM images of areas (d) B and (e) A representing respectively to dc flux-free and flux-captured states at $f = 18.845$ GHz.

response of the meta-surface at $f = 18.57$ GHz [see Fig. 3(c) and the inset in Fig. 3(a)] similar to that theoretically predicted assuming nearest neighbor coupling in a 2D array of rf-SQUIDs [24]. The resonance of 18.57 GHz shows a clear periodicity with dc flux starting from $\Phi_{dc}/\Phi_0 = 0$ up to the highest value of 10, as measured in a zero-field-cooled sample. However, the result was dramatically changed when cooling was done in a weak magnetic field. In this case, dc flux was trapped in the lattice of the rf-SQUID array locally despite the fact that cooling is being conducted in a spatially homogenous dc field [see Fig. 5(e)]. Magnetic flux dependence of zero-field cooled rf-SQUID array in the magneto-inductive mode of $f = 18.845$ GHz is shown in Fig. 5(a) by the blue solid line. Again, the response is periodic with the dc flux and the 2D LSM photo-response has been measured at flux point 1, and demonstrated the predicted coherent excitation, as seen in Fig. 5(b).

The homogenous field cooled sample shows a modified pattern of PR vs. Φ_{dc}/Φ_0 having zero response at $\Phi_{dc}/\Phi_0 = 0$ while the maximum of LSM PR is relocated to $\Phi_{dc}/\Phi_0 = +/- 0.5$ similar to the case of the critical-current pattern in a single JJ [25]. The $PR(x,y)$ is enhanced in a ring of four JJs as seen in area A of Fig. 5(c) and in the enlarged image of Fig. 5(e). This feature is due to the increase of their Josephson inductance by the screening current flow directed along the edge of hole outlined in Fig. 5(d) as a reference. It is interesting that the other JJs in the array remain in coherent response as one can see from Fig. 5(d) showing the $PR(x,y)$ distribution in area B. This may be understood as a result of destroyed coupling of individual SQUIDs in the array.

IV. SUMMARY

We have shown the effect of spatial redistribution of microwave response in the array of 27x27 coupled SQUIDs under the influence of a tuned homogenous dc flux. Unexpected magneto-inductive modes were found in the high rf flux limit. We demonstrated that the LSM technique is a very successful tool for spatially-resolved characterization of complicated meta-materials and may be useful for study of the physics underlying its unusual microwave properties.

References

- [1] J. B. Pendry, A. J. Holden, D. J. Robbins, and W. J. Stewart, "Magnetism from conductors and enhanced nonlinear phenomena," *IEEE Trans. Microw. Theory Tech.*, vol. 47, pp. 2075–2084, Nov. 1999.
- [2] C. L. Holloway, E. F. Kuester, J. A. Gordon J. O'Hara, J. Booth, D. R. Smith, "An Overview of the Theory and Applications of Metasurfaces: The Two-Dimensional Equivalents of Metamaterials," *IEEE Antennas and Propagation Magazine*, vol. 54, pp.10-35, April 2012.
- [3] M. Ricci, N. Orloff, and S. M. Anlage, "Superconducting metamaterials," *Appl. Phys. Lett.* vol. 87, pp. 034102 (1-3), July 2005.
- [4] P. Jung, A. V.Ustinov, and S.M.Anlage, "Progress in superconducting metamaterials," *Supercond. Sci. Technol.*, vol. 27, pp. 073001 (1-13), May 2014.
- [5] C. Du, H. Chen, and S. Li, "Quantum left-handed metamaterial from superconducting quantum-interference devices", *Phys. Rev. B*, vol. 74, pp. 113105 (1-4), Sept. 2006.
- [6] N. Lazarides and G. P. Tsironis, "rf superconducting quantum interference device metamaterials," *Appl. Phys. Lett.*, vol. 90, 163501(1-3), April 2007.
- [7] A. I. Maimistov, I. Gabitov, "Nonlinear response of a thin metamaterial film containing Josephson junctions," *Opt. Commun.* vol. 283, pp. 1633-1639, April 2010.
- [8] M. Trepanier, "Tunable Nonlinear Superconducting Metamaterials: Experiment and simulation," Ph.D. thesis, University of Maryland, 2015, <http://drum.lib.umd.edu/handle/1903/17290>.
- [9] A. V. Ustinov, "Experiments With Tunable Superconducting Metamaterials," *IEEE Transact. Terahertz Sci. and Technol.*, vol. 5, pp. 22-26, Jan, 2015.
- [10] M. Trepanier, D. Zhang, O. Mukhanov, and S. M. Anlage, "Realization and Modeling of Metamaterials Made of rf Superconducting Quantum-Interference Devices," *Phys. Rev. X*, vol. 3, pp. 041029 (1-11), Dec. 2013.
- [11] P. Jung, S. Butz, S. V. Shitov, and A. V. Ustinov, "Low-loss tunable metamaterials using superconducting circuits with Josephson junctions," *Appl. Phys. Lett.*, vol. 102, pp. 062601 (1-3), Feb. 2013.
- [12] D. Zhang, M. Trepanier, O. Mukhanov, and S. M. Anlage, "Tunable Broadband Transparency of Macroscopic Quantum Superconducting Metamaterials," *Phys. Rev. X*, vol. 5, pp. 041045(1-6), Dec. 2015
- [13] N. Lazarides, G. Neofotistos, and G. P. Tsironis, "Chimeras in squid metamaterials," *Phys. Rev. B*, vol. 91, pp. 054303 (1-8), Feb. 2015.
- [14] N. Lazarides and G. P. Tsironis, "Multistability and self-organization in disordered SQUID metamaterials," *Supercond. Sci. Technol.*, vol. 26, pp. 084006(1-10), July 2013.
- [15] P. Jung, R. Kosarev, A. Zhuravel, S. Butz, V. Koshelets, L. V. Filippenko and A. V. Ustinov, "Imaging the electromagnetic response of superconducting metasurfaces," in *Proc. Metamater. 2013*, Bordeaux, France, pp. 1-3, Sept. 2013.
- [16] D. Yohannes, A. Kirichenko, S. Sarwana, and S. K. Tolpygo, "Parametric testing of HYPRES superconducting integrated circuit fabrication processes," *IEEE Trans. Appl. Supercond.*, vol. 17, pp. 181-186, June 2007.
- [17] B. Chesca. Theory of RF SQUIDs operating in the presence of large thermal fluctuations. *J. Low Temp. Phys.*, vol. 110, pp. 963-1001, March 1998.
- [18] A. S. Averkin, A. P. Zhuravel, P. Jung, N. Maleeva, V. P. Koshelets, L. V. Filippenko, A. Karpov, and A. V. Ustinov, "Imaging coherent response of superconducting metasurface," *IEEE Trans. Appl. Supercond.*, vol. 26, pp. 1-3, Jan. 2016.
- [19] A. P. Zhuravel, S. M. Anlage, and A. V. Ustinov, "Imaging of Microscopic Sources of Resistive and Reactive Nonlinearities in Superconducting Microwave Devices," *IEEE Trans. Appl. Supercond.*, vol. 17, pp. 902 – 905, June 2007.
- [20] A. P. Zhuravel, C. Kurter, A.V. Ustinov, and S. M. Anlage, "Unconventional rf photoresponse from a superconducting spiral resonator," *Phys. Rev. B*, vol. 85, pp. 134535 (1-8), April 2012.
- [21] A. P. Zhuravel, S. M. Anlage, and A. V. Ustinov, "Measurement of local reactive and resistive photoresponse of a superconducting microwave device," *Appl. Phys. Lett.*, vol. 88, pp. 212503 (1-3), May 2006.
- [22] A.P. Zhuravel, A. G. Sivakov, O. G. Turutanov, A. N. Omelyanchouk, S. M. Anlage, A. Lukashenko, A.V. Ustinov, and D. Abraimov, "Laser scanning microscopy of HTS films and devices," *Low Temp. Phys.* vol. 32, pp. 592-607, June 2006.
- [23] G. P. Tsironis, N. Lazarides, and M. Eleftheriou, "Dissipative Breathers in rf SQUID Metamaterials," *PIERS Online Vol. 5*, pp: 26-30, 2009.
- [24] G. P. Tsironis, N. Lazarides, and I. Margaris, "Wide-band tuneability, nonlinear transmission, and dynamic multistability in SQUID metamaterials," *Appl. Phys. A*, Vol. 117pp. 579-588, Nov. 2014.
- [25] A. Franz, A. Wallraff, and A. V. Ustinov, "Measurements of critical-current diffraction patterns in annular Josephson junctions," *Phys. Rev. B*, vol. 62, pp. 119-122, July 2000.